Algorithms and Challenges of Electron Microscope Tomography

Gregory Beylkin

IPAM
January 29, 2008

CU BOULDER

Current Algorithms

In 2003 Kristian Sandberg, David N. Mastronarde and I published a paper "A fast reconstruction algorithm for electron microscope tomography" in J. of Structural Biology, v. 144. The algorithm uses the Fourier domain to gain speed. Our main goal was to match the accuracy of the usual backprojection algorithm and increase speed (which we did, it is for a number of years a part of IMOD package).

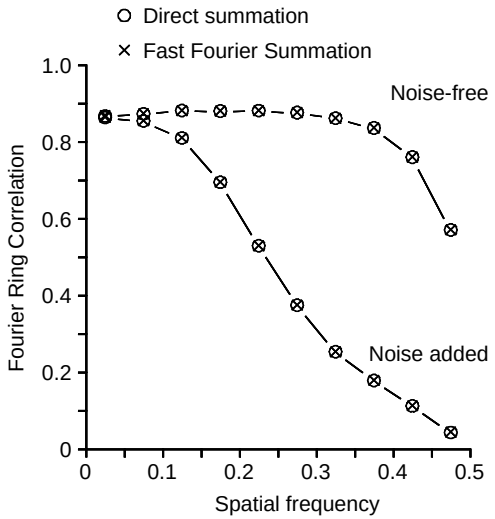

Total speed up was about a factor of 30, but most of the gain (a factor of 10) came from .....

It may be time to revise a reconstruction algorithm written in the 70s ... not a simple task ...

Challenges of Electron Microscope Tomography

1. The imaging technique is hardly "non-destructive"; a limited useful energy range.

2. Limited aperture resulting in artifacts, very noisy data

3. Difficulties with forward modeling

4. ....

Currently we are looking at a number of new mathematical tools to address several challenges of NDE imaging in general and electron microscopy in particular.

The rest of my talk is a mathematical desription of our approach and tools at our disposal.

This work involves Kristian Sandberg, Lucas Monzón, Christopher Kurcz and (recently) Matt Reynolds.

Fourier transform on a finite domain

It is well-known that a function with compactly supported Fourier transform cannot have compact support itself unless it is identically zero.

Yet, all measurements, being approximate, violate this localization constraint since we never deal with either infinite bandwidth nor with functions that extend indefinitely in space or time.

This constraint is easily overcome for a finite accuracy. For example, consider a Gaussian and set a threshold on the function and its Fourier transform, thus limiting both supports for any finite accuracy.

Thus, it is natural to analyze the operator whose effect on a function is to truncate it both in spatial and Fourier domains. This has been the topic of a series of seminal papers by Slepian et al. (circa 1961), where it is observed ($inter\ alia$) that the eigenfunctions of such operator on a finite interval are the Prolate Spheroidal Wave Functions (PSWFs) of classical mathematical physics.

Bases born on an interval: Slepian's (PSWF) functions

The PSWFs are the eigenfunctions of the operator

$$F_c(\psi_j)(x) = \lambda_j \psi_j(x),$$

where $F_c : L^2[-1,1] \to L^2[-1,1]$,

$$F_c(\phi)(x) = \int_{-1}^{1} e^{icx\xi} \phi(\xi) d\xi,$$

and c is a positive real constant (bandlimit).

The eigenvalues λ_j, $j = 0, 1, \ldots$, are all non-zero and simple, and are arranged so that $|\lambda_j| > |\lambda_{j+1}|$.

Each λ_j is either real or pure imaginary, according to the parity of the eigenfunction ψ_j.

Band-limiting and time-limiting operator

The eigenfunctions ψ_j are also eigenfunctions of the band-limiting and time-limiting operator $Q_c = \frac{c}{2\pi} F_c^* F_c$,

$$Q_c(\psi_j)(x) = \frac{1}{\pi} \int_{-1}^{1} \frac{\sin c(x-y)}{x-y} \psi_j(y) dy = \mu_j \psi_j(x),$$

with eigenvalues

$$\mu_j = \frac{c}{2\pi} |\lambda_j|^2, \quad j = 0, 1, \ldots$$

For large c the first $\approx 2c/\pi$ eigenvalues μ_j are close to 1.

Then the next $\mathcal{O}(\log c)$ eigenvalues decay exponentially fast to almost zero.

The rest of the eigenvalues are very close to zero.

Where the name "PSWFs" comes from?

There exists a strictly increasing sequence of real numbers $\eta_0 < \eta_1 < \dots$, such that ψ_j are eigenfunctions of the differential operator

$$L\psi_j \equiv \left(-(1-x^2)\frac{d^2}{dx^2} + 2x\frac{d}{dx} + c^2x^2\right)\psi_j(x) = \eta_j\psi_j(x).$$

The eigenfunctions of L have been known as the angular prolate spheroidal functions.

About 50 years ago Slepian et.al. discovered that L and F_c commute and constructed a useful theory for bandlimited functions.

We note that if $c \to 0$ then, in this limit, PSWFs ψ_j become the Legendre polynomials.

Also, for any $n \geq 0$, the first n functions ψ_j, $j = 0, \dots, n-1$, form a Chebyshev system. In particular, the number of zeros of ψ_j in $[-1, 1]$ is equal to j.

Important properties of PSWFs

Defined on the interval $[-1,1]$, PSWFs ψ_j are extended to the real line via

$$\psi_j(x) = \frac{1}{\mu_j \pi} \int_{-1}^{1} \frac{\sin c(x-y)}{(x-y)} \psi_j(y) dy.$$

These functions are orthogonal on both $[-1,1]$ and the real line $(-\infty,\infty)$,

$$\int_{-1}^{1} \psi_j(x)\, \psi_l(x)\, dx = \delta_{jl} \quad \text{and} \quad \int_{-\infty}^{\infty} \psi_j(x)\, \psi_l(x)\, dx = \frac{1}{\mu_j} \delta_{jl}.$$

We have the optimal separated representation for the exponential,

$$e^{icxy} = \sum_{j=0}^{\infty} \lambda_j\, \psi_j(x) \psi_j(y)\,.$$

Recent results: Gaussian-type quadratures for bandlimited functions

Currently there are two methods for finding nodes and weights to integrate functions e^{ibx} for $|b| \leq c$ with user selected accuracy ϵ:

- Since the first n PSWFs form a Chebyshev system, the generalized Gaussian quadratures for PSWFs can be constructed numerically. For a given accuracy ϵ and a choice of n, these quadratures are also quadratures for exponentials. This approach has been taken in *Xiao-Rokhlin-Yarvin*, Inverse Problems, 2001

- We have constructed a new type of the generalized Gaussian quadratures directly for exponentials in *Beylkin-Monzón*, Appl. & Comp. Harm. Anal., v. 12, 2002. These quadratures are parameterized by eigenvalues of the Toeplitz matrix constructed from the trigonometric moments of a positive measure. For a given accuracy ϵ, selecting an eigenvalue close to ϵ and the corresponding eigenvector yields (in the end) an approximate quadrature for that accuracy.

Distribution of nodes of Gaussian quadratures

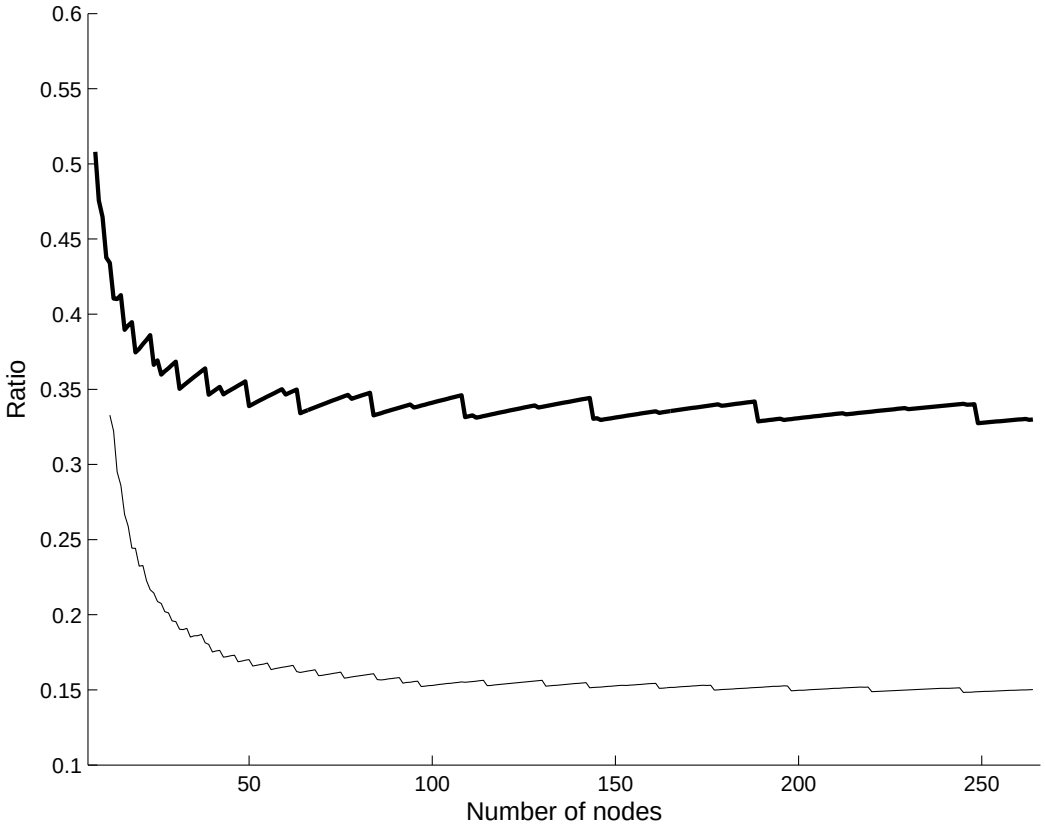

The ratio $r(M,\epsilon) = \frac{\theta_2 - \theta_1}{\theta_{\lfloor M/2 \rfloor} - \theta_{\lfloor M/2 \rfloor - 1}}$ plotted against the number of nodes for quadratures of accuracy $\epsilon \approx 10^{-7}$ and $\epsilon \approx 10^{-17}$.

Sampling rate for Gaussian quadratures

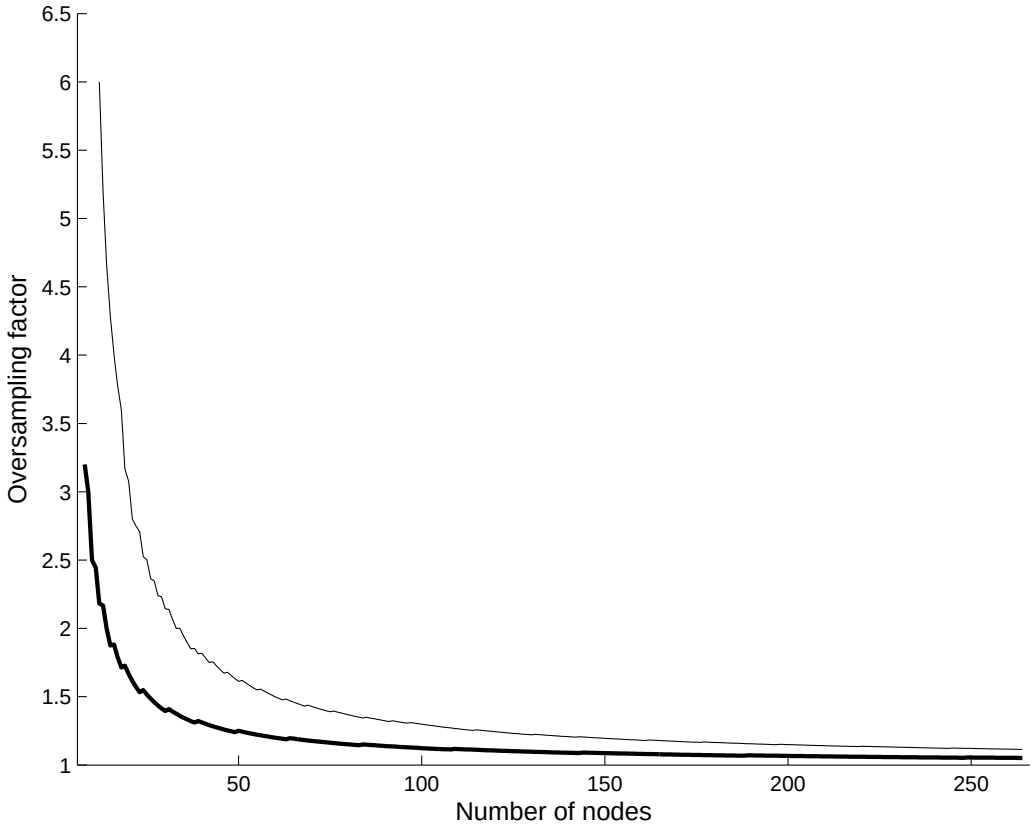

The oversampling factor $\alpha(M,\epsilon) = \frac{\pi M}{c(M,\epsilon)} > 1$ plotted against the number of nodes for quadratures of accuracy $\epsilon \approx 10^{-7}$ and $\epsilon \approx 10^{-17}$.

Accuracy of the Gaussian quadratures

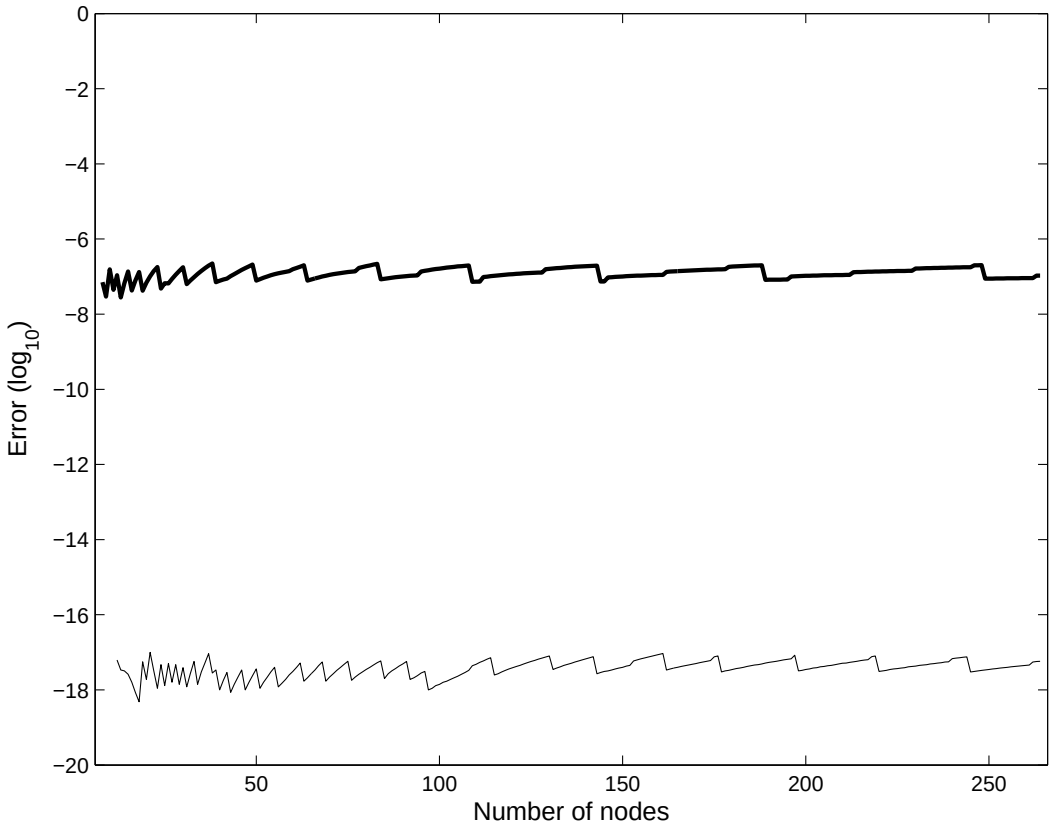

Accuracy ϵ of the Gaussian quadratures for integration. For interpolation accuracy is $\sqrt{\epsilon}$.

Comparison of derivative operators

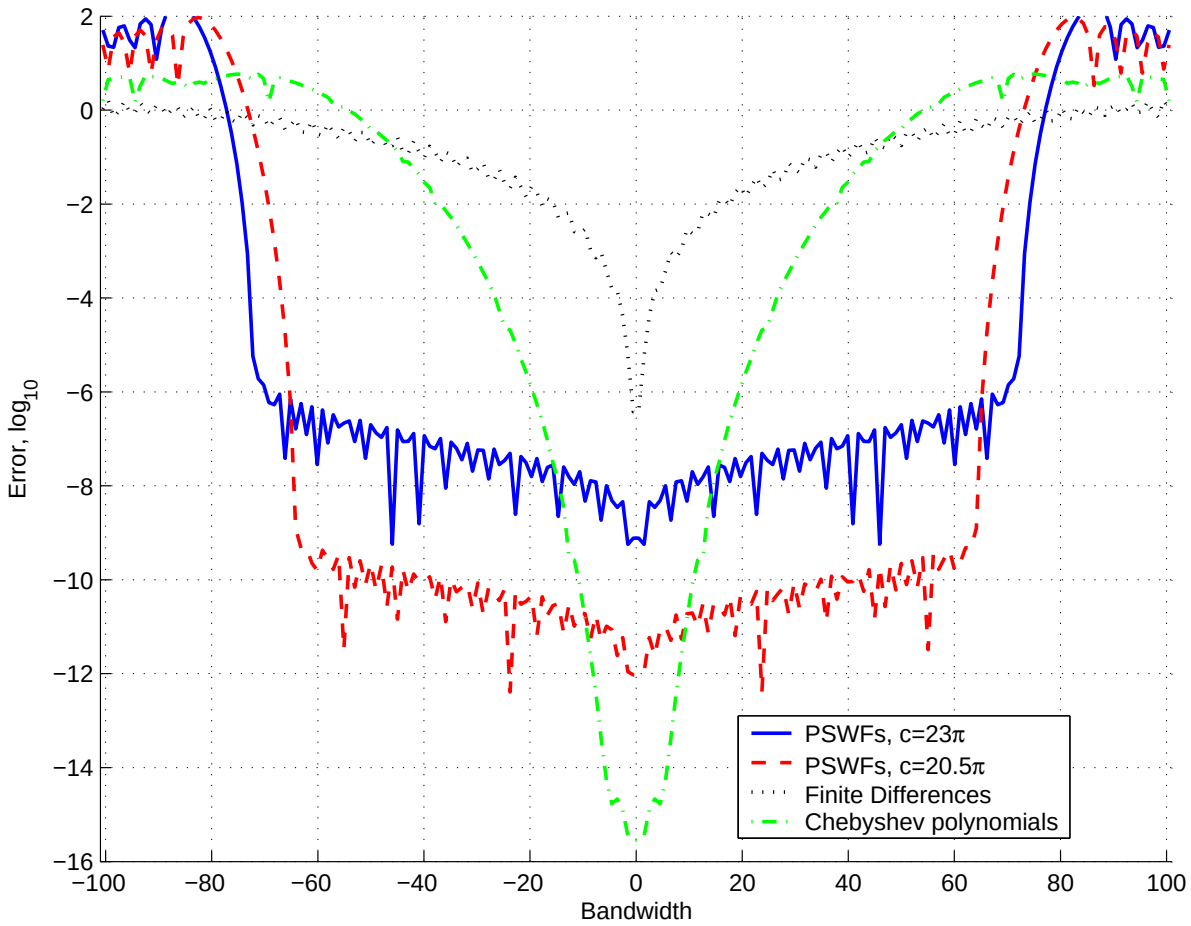

Error of differentiating $\sin(bx)$ for $|b| \leq 32\pi$ on the interval $[-1, 1]$ using PSWFs with 64 nodes, 4th-order FD and the Chebyshev polynomials of degrees up to 15 on 4 subintervals.

Slepian functions in higher dimensions

Slepian (1964) also considered mapping of a disk in space to a disk in the Fourier domain (or a ball in higher dimension).

However, the spectrum of the space-limiting and band-limiting operator for the disk-to-disk mapping is substantially different from that in 1D. Namely, the complete spectrum has a large transition region (of order $\mathcal{O}(N \log N)$ out of $\mathcal{O}(N^2)$ eigenvalues).

Recently Yoel Shkolnisky implemented Slepian's construction. For each angular mode the transition region is $\mathcal{O}(\log N)$, but there are $\mathcal{O}(N)$ angular modes!

Transforms from square in space to a disk in Fourier domain (and back)

- A really long list of applications which include the Radon transform and its practical variants
- Note that the pseudo-polar DFT maps a square in space to a square in Fourier domain but with a radial grid
- Directional bases, curvelets, etc.

Is there a "correct" mathematical object, an analogue of DFT, or this is just numerics?

What are "good" grids in a disk?

Forward and adjoint transforms

Consider the Fourier transform of a function f supported in B,

$$\hat{f}(\mathbf{p}) = \mathcal{F}_{2c}[f](\mathbf{p}) = \int_B f(\mathbf{x}) e^{-i\mathbf{x}\cdot\mathbf{p}} d\mathbf{x},$$

and restrict the support of $\hat{f}$ to the disk of radius $2c$, so that

$$\mathcal{F}_{2c} : L^2(B) \to L^2(D_{2c}).$$

We then consider the adjoint transform

$$\mathcal{F}_{2c}^*[\hat{g}](\mathbf{x}) = \frac{1}{4\pi^2} \int_{D_{2c}} \hat{g}(\mathbf{p}) e^{i\mathbf{x}\cdot\mathbf{p}} d\mathbf{p},$$

and limit the support of the resulting function to the square B, so that

$$\mathcal{F}_{2c}^* : L^2(D_{2c}) \to L^2(B).$$

Slepian operator

We now define the band-limiting and space-limiting operator as

$$\mathcal{Q}_{2c} = \mathcal{F}_{2c}^* \mathcal{F}_{2c} : L^2(B) \to L^2(B),$$

where $\mathcal{Q}_{2c}[f](\mathbf{x}) = \frac{1}{4\pi^2} \int_{D_{2c}} \hat{f}(\mathbf{p}) e^{i\mathbf{x}\cdot\mathbf{p}} d\mathbf{p}$. The compact positive definite operator $\mathcal{Q}_{2c}$ acts as a convolution with kernel

$$K_{2c}(\mathbf{x}) = K_{2c}(x_1, x_2) = \frac{1}{4\pi^2} \int_{D_{2c}} e^{i\mathbf{p}\cdot\mathbf{x}} d\mathbf{p} = \frac{c\, J_1(2c\sqrt{x_1^2 + x_2^2})}{\pi\sqrt{x_1^2 + x_2^2}},$$

and we consider the eigenvalue problem

$$\mu_j \psi_{j,2c}(\mathbf{y}) = \int_B K_{2c}(\mathbf{y} - \mathbf{z})\, \psi_{j,2c}(\mathbf{z})\, d\mathbf{z},$$

where $\mathbf{y}, \mathbf{z} \in B$, $j = 0, 1, 2, \ldots$ and $1 > \mu_0 > \mu_1 \geq \mu_2 \geq \ldots$.

Spectrum of space-limiting and band-limiting operator for square to disk mapping

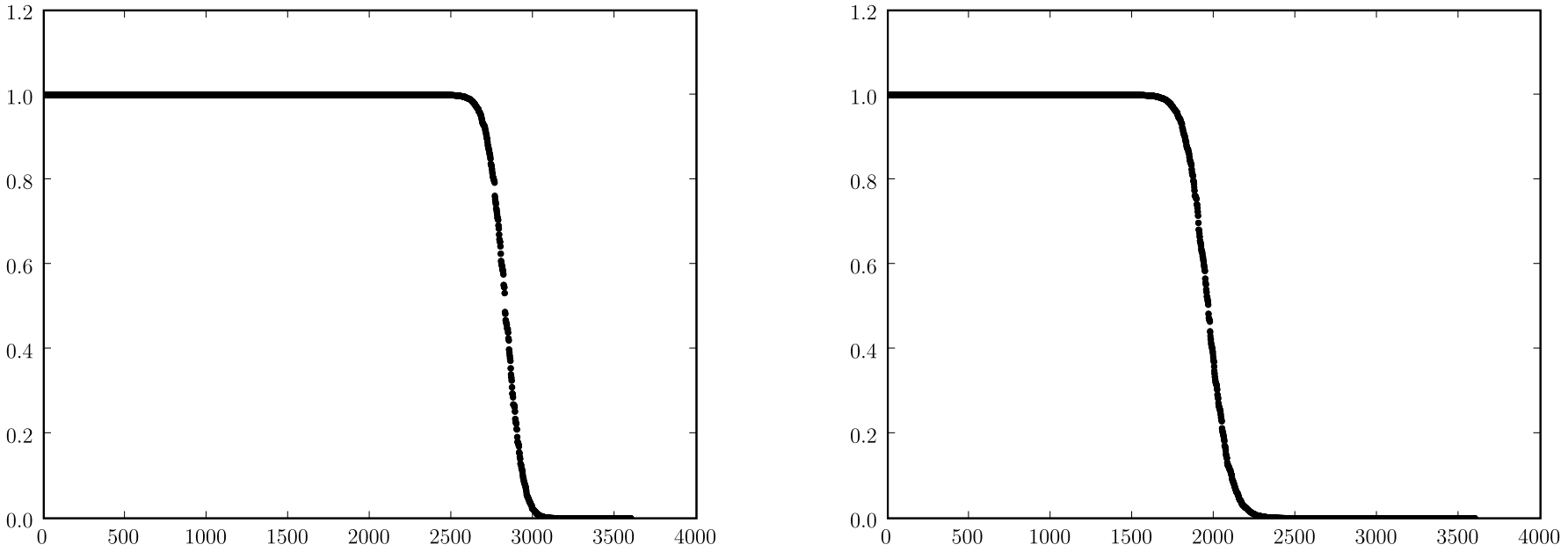

Eigenvalues of space-limiting and band-limiting operator for equally and unequally spaced discretization in space ($N = N_\omega = 60$).

Eigenvectors in the "effective null space"

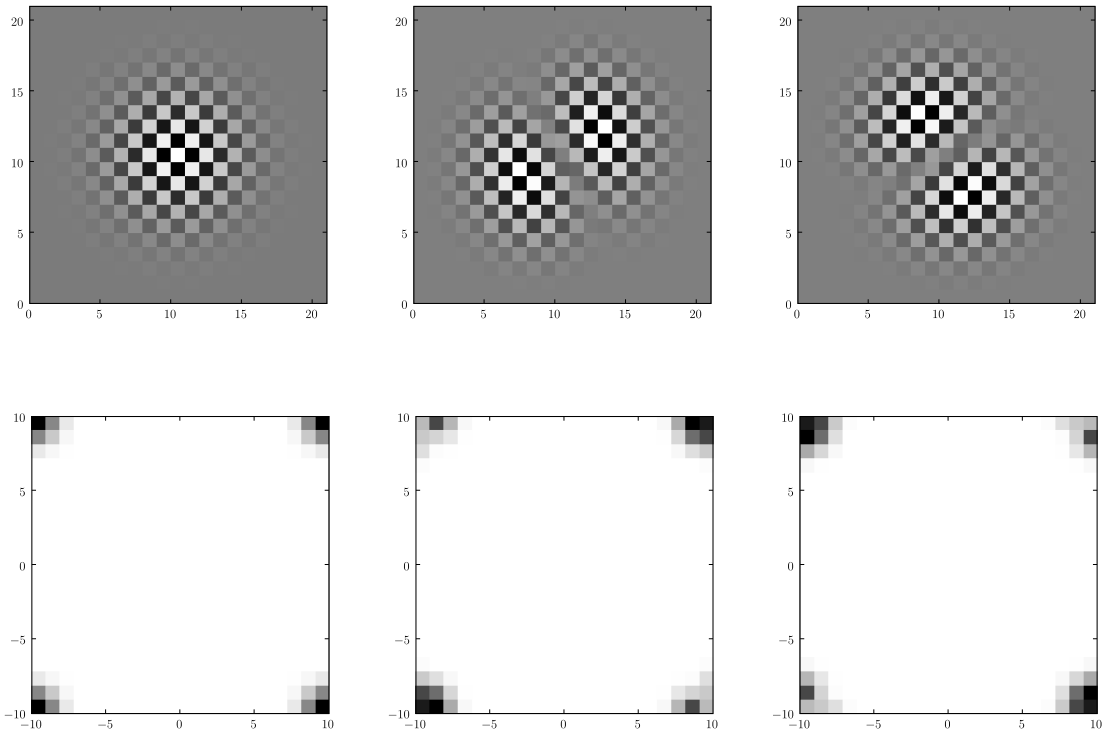

The last three eigenvectors of (top row) and the magnitude of their discrete Fourier transforms (bottom row) for $N = 21$.

Quadratures: nodes and weights on the diameter of the disk

We compute for given $\epsilon > 0$ and bandlimit $2\sqrt{2}c > 0$ the nodes $|\rho_k| < 1$ and the weights $w_k > 0$, $k = 1, \ldots, M$, where $M = M(c, \epsilon)$, such that for all $y \in [-1, 1]$

$$\left| \int_{-1}^{1} e^{i\,2\sqrt{2}c\rho y}\,|\rho|\,d\rho - \sum_{k=1}^{M} w_k e^{i\,2\sqrt{2}c\rho_k y} \right| \leq \frac{\pi\epsilon}{c^2}.$$

With these we obtain a discretization of the kernel,

$$\begin{aligned} K_{2c}(\mathbf{x}) &= \frac{c^2}{\pi^2} \int_0^{2\pi} \int_0^1 e^{i\,2c\,\rho(x_1\cos\theta + x_2 \sin\theta)} \rho\,d\rho\,d\theta \\ &= \frac{c^2}{2\pi^2} \int_0^{2\pi} \left(\int_{-1}^{1} e^{i\,2c\,\rho(x_1\cos\theta + x_2 \sin\theta)} |\rho|\,d\rho \right) d\theta. \end{aligned}$$

Example of nodes and weights on the diameter

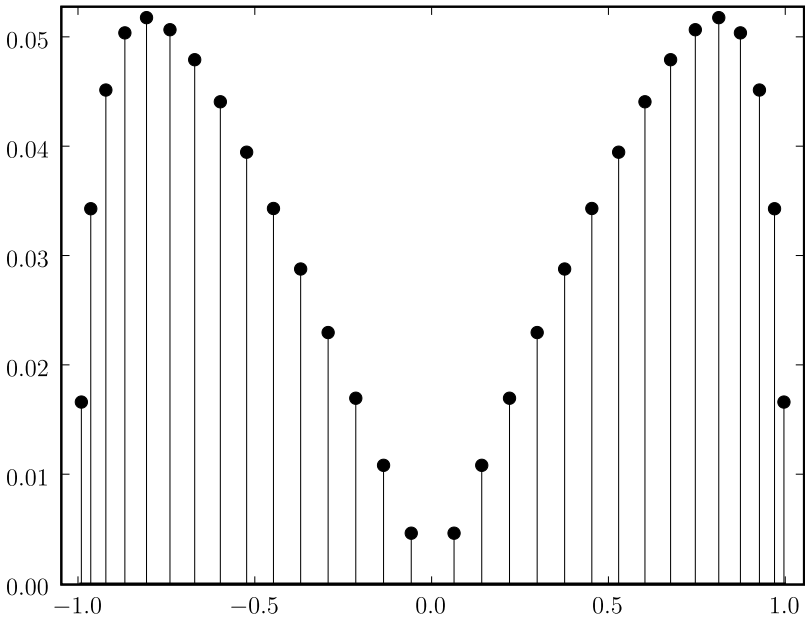

Weights at radial nodes for $M = 30$, $\epsilon \approx 9.75 \cdot 10^{-6}$ and $c \approx 23.324$. As expected, the weights mimic the measure $|\rho| d\rho$.

Inversion on a subspace

Consider

$$\mathbf{f} = \sum_{j=0}^{N_\omega^2-1} \langle \mathbf{f}, \psi_j^\omega \rangle_\omega \psi_j^\omega.$$

For a given accuracy $\delta > 0$, split the spectrum of Slepian operator into three parts $J_{head} = \{j \in \mathbb{N} \,|\, \mu_j^\omega > 1-\delta\}$, $J_{decay} = \{j \in \mathbb{N} \,|\, 1-\delta \geq \mu_j^\omega \geq \delta\}$, and $J_{tail} = \{j \in \mathbb{N} \,|\, \mu_j^\omega < \delta\}$.

We assume that $\mathbf{f}$ has a small projection on the eigenvectors of the tail region,

$$\left(\sum_{j \in J_{tail}} |\langle \mathbf{f}, \psi_j^\omega \rangle_\omega|^2 (1-\mu_j^\omega)^2 \right)^{1/2} \leq \delta \|\mathbf{f}\|_\omega.$$

Inversion algorithm

Given $\mathbf{f}^\sharp = G_{\omega,2c}[\mathbf{f}]$, where $G_{\omega,2c}$ is the forward transform, we would like to recover $\mathbf{f}$ (under the assumption).

Assume that the functions ψ_j^ω and $\psi_j^{\sharp,\omega}$ for indices $j \in J_{decay}$ have been computed in advance. We compute

1. $\alpha_j = \left\langle \mathbf{f}^\sharp, \psi_j^{\sharp,\omega} \right\rangle_\sigma$ for indices in J_{decay}.

2. Given α_j and the eigenvalues μ_j^ω, we form

$$\mathbf{d} = \sum_{j \in J_{decay}} \frac{\alpha_j}{\mu_j^\omega} \psi_j^\omega \quad \text{and} \quad \mathbf{d}^\sharp = \sum_{j \in J_{decay}} \frac{\alpha_j}{\mu_j^\omega} \psi_j^{\sharp,\omega}.$$

   We note that $G_{\omega,2c}(\mathbf{d}) = \mathbf{d}^\sharp$.

3. As an approximation to $\mathbf{f}$ we compute

$$\mathbf{f}_{recon} = G^*_{\omega,2c}[\mathbf{f}^\sharp - \mathbf{d}^\sharp] + \mathbf{d}.$$

Rotation of a function

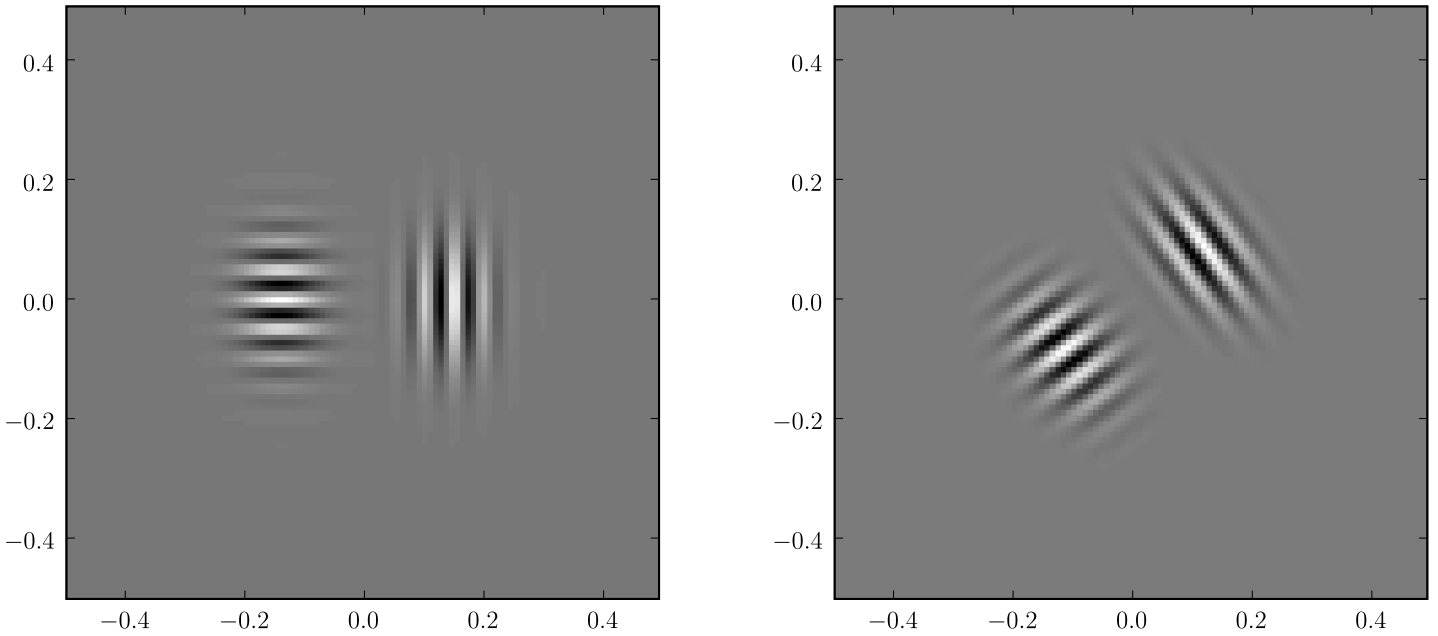

$$f(x_1, x_2) = e^{-\sigma_1 (x_1 - \tau)^2} e^{-\sigma_2 x_2^2} \cos(k x_1) + e^{-\sigma_1 (x_1 + \tau)^2} e^{-\sigma_2 x_2^2} \cos(k x_2),$$

with $k = 40\pi$, $\sigma_1 = 240$, $\sigma_2 = 100$ and $\tau = 1/7$. The rotation is by $\phi = \pi/5$ with accuracy $\approx 1.33 \cdot 10^{-11}$.

Inversion via a fast algorithm

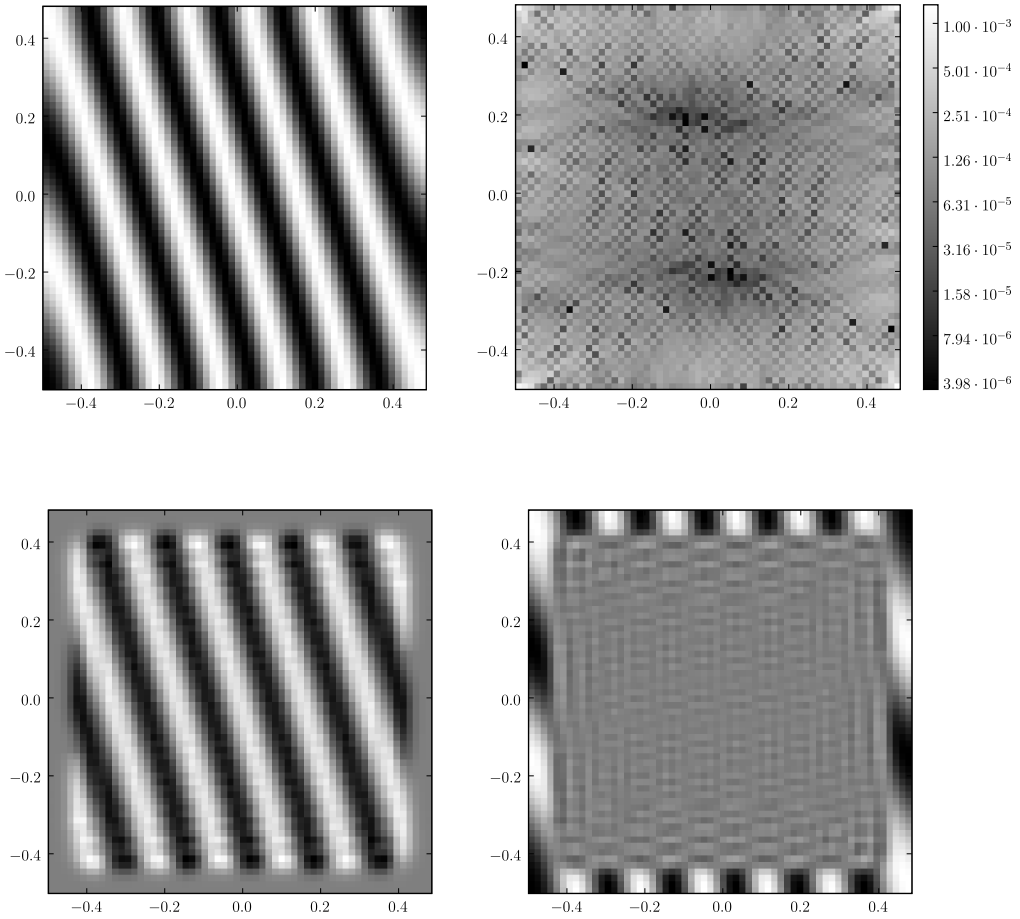

Rotating Grid

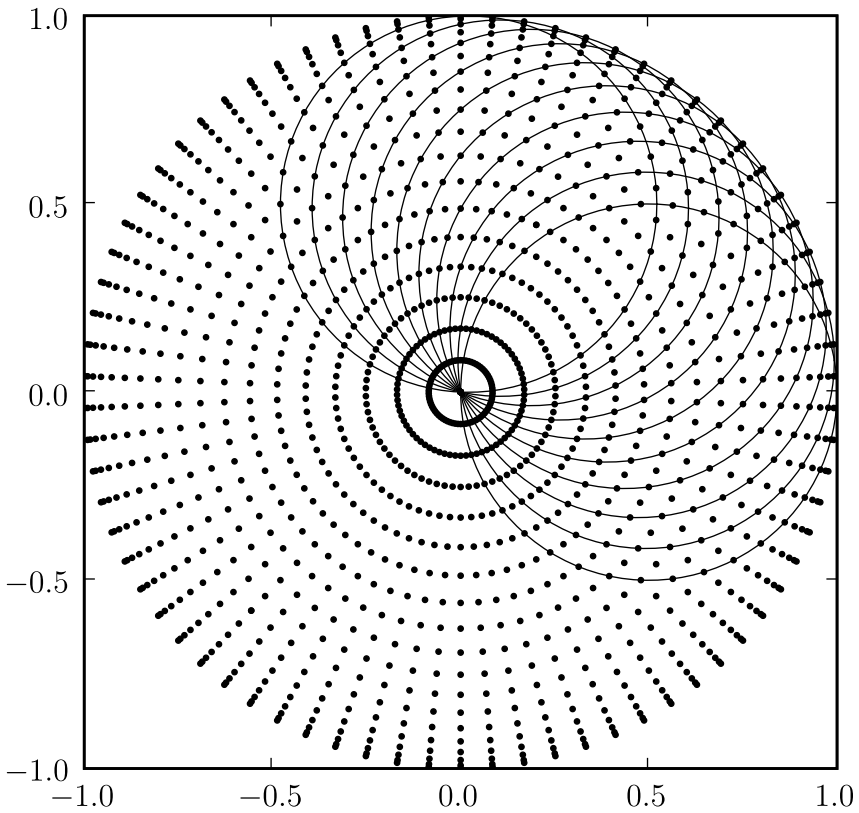

Grids with even and odd subdivisions

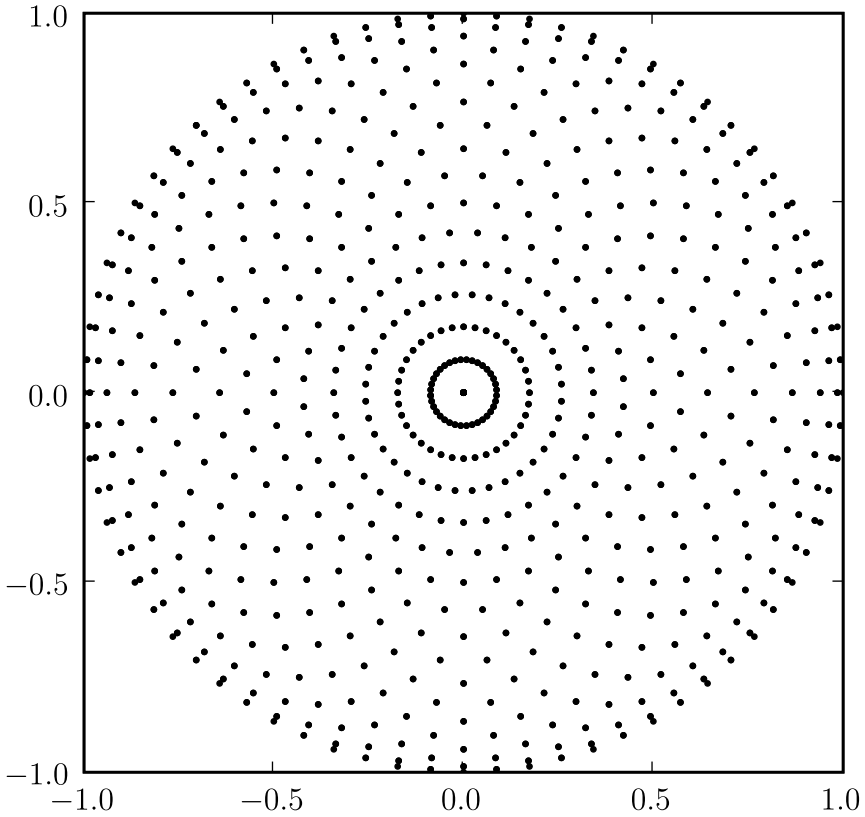

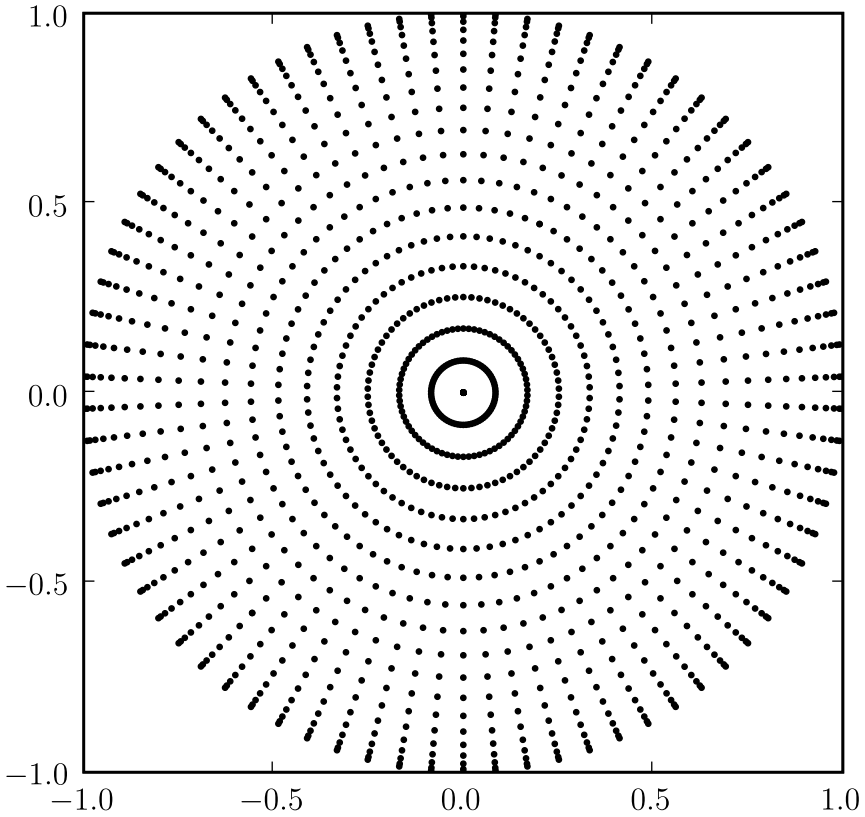

Grids with even $N_\alpha = N_\beta = 36$ and odd $N_\alpha = N_\beta = 37$ number of points.

Trigonometric interpolation on circles in the Fourier domain

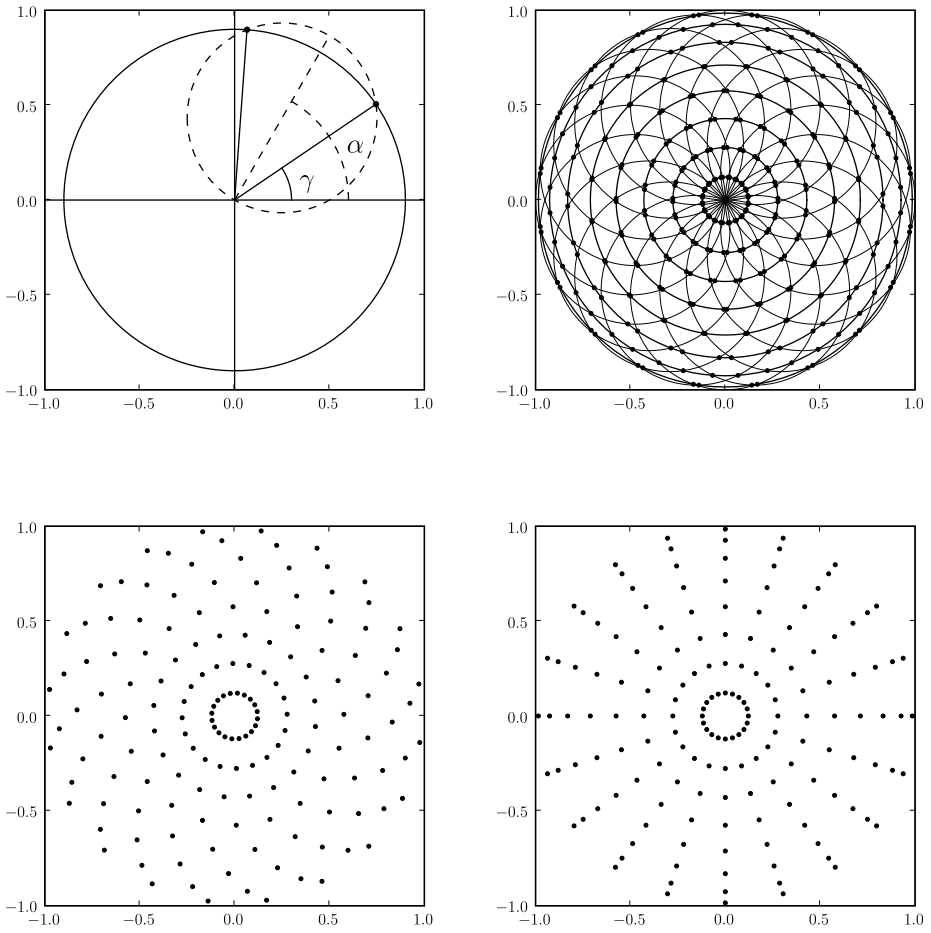

Imbeded Grids

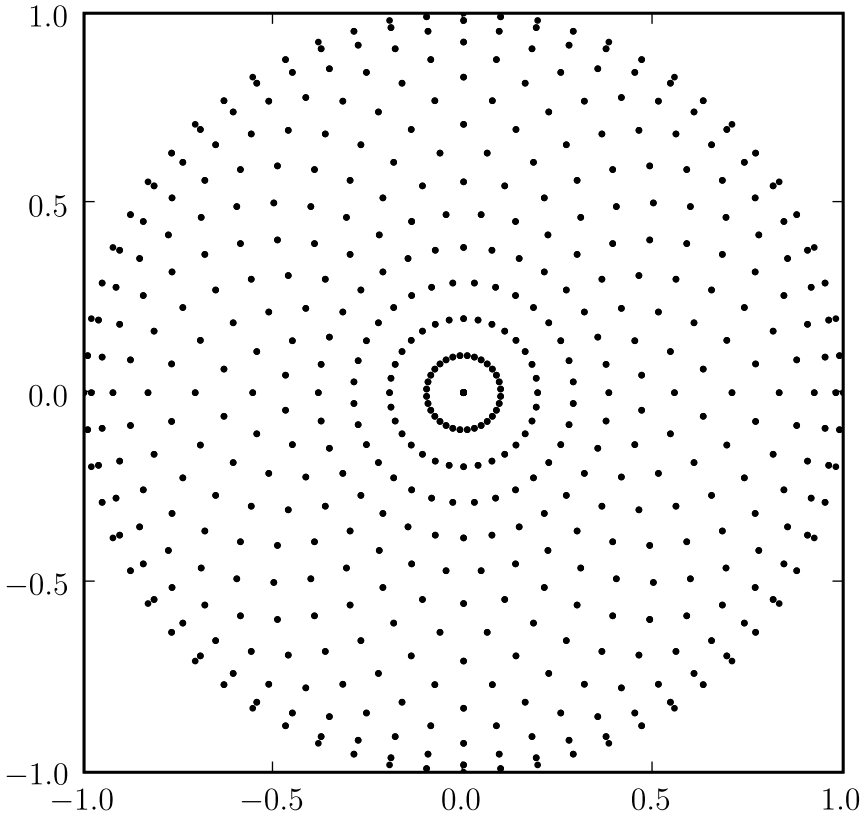

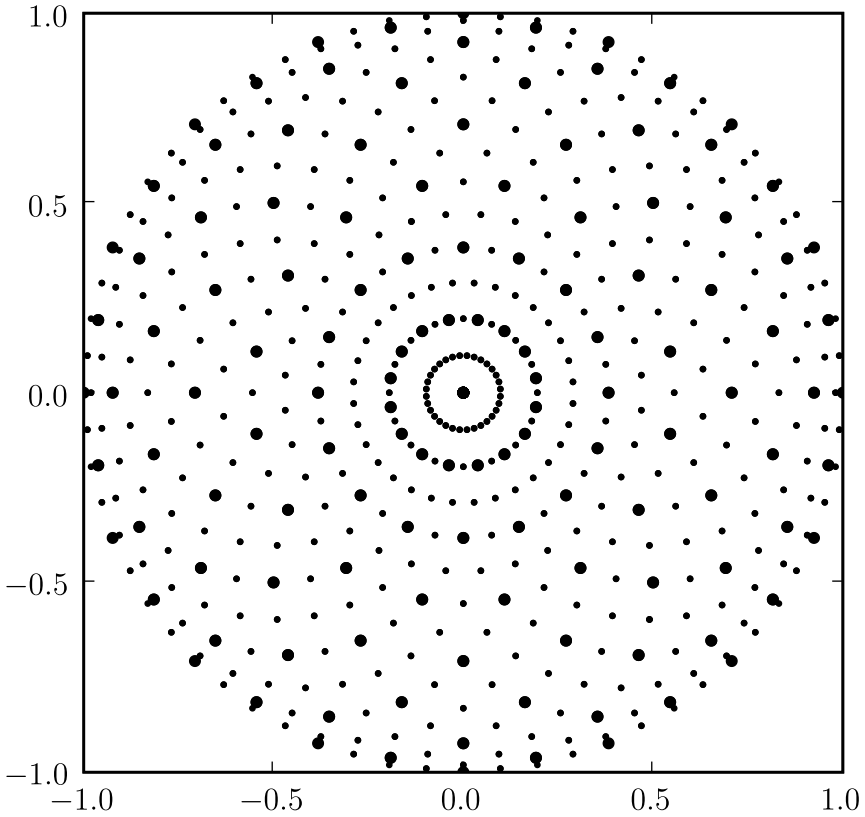

Experiments to reduce the effect of limited aperture

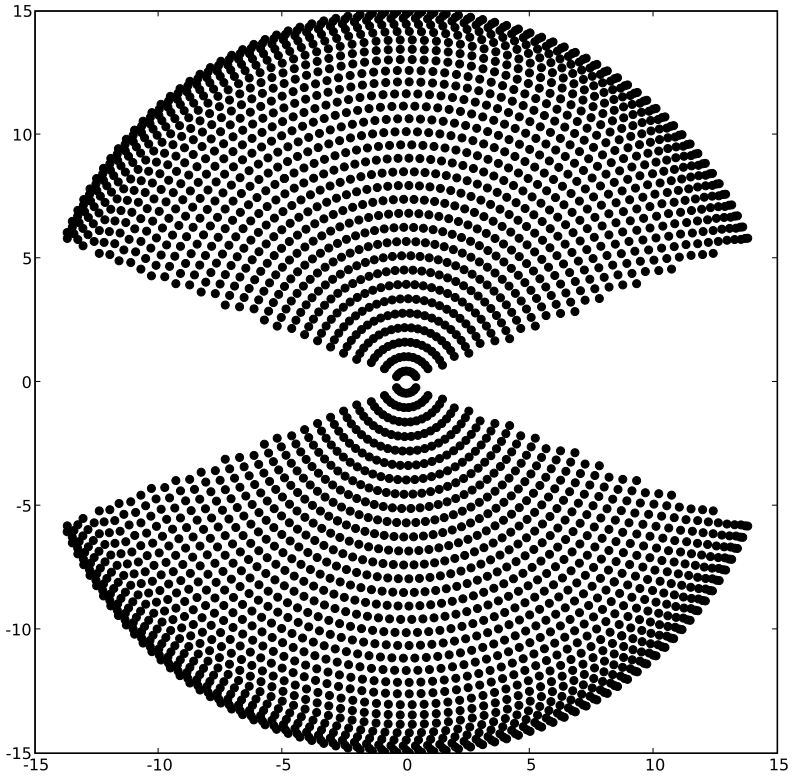

Example of a missing wedge

Simple test

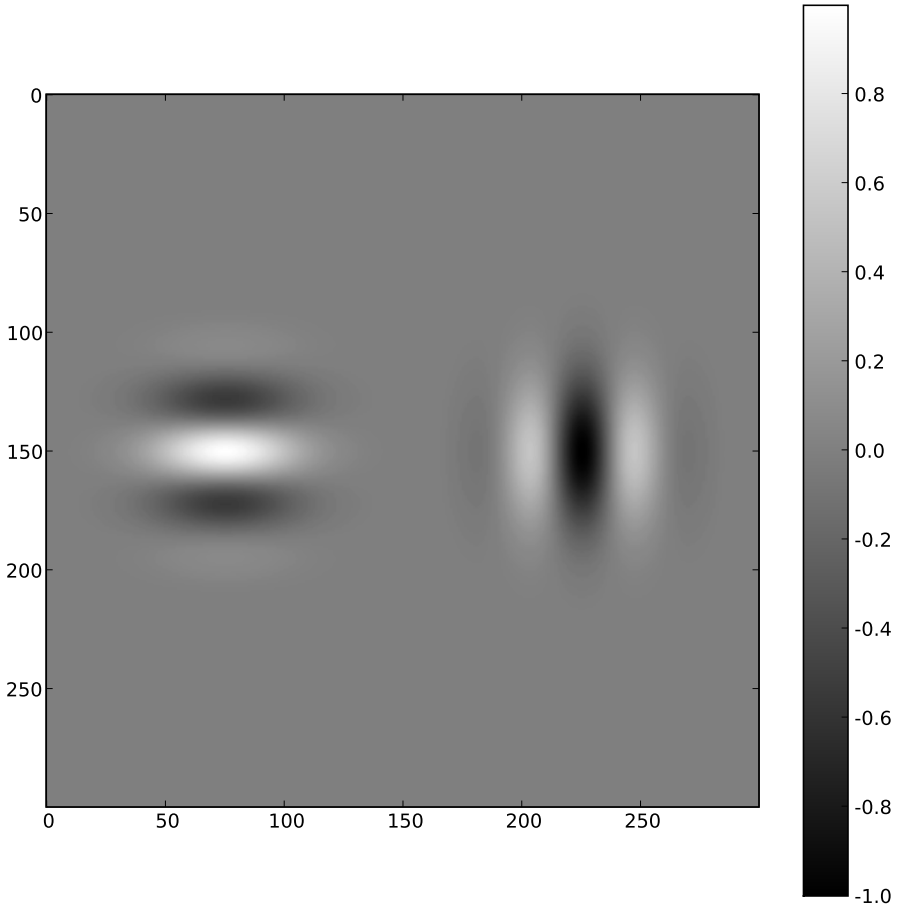
0
50
100
150
200
250
0
50
100
150
200
250
0.8
0.6
0.4
0.2
0.0
-0.2
-0.4
-0.6
-0.8
-1.0

Reconstruction

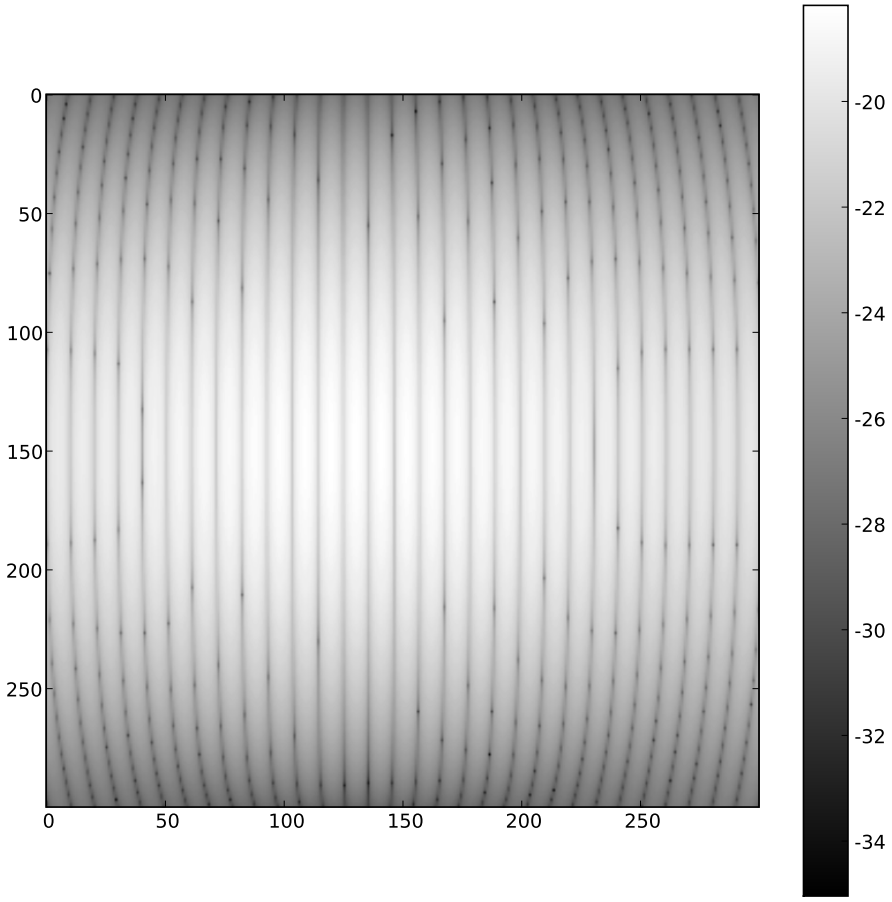

Error of reconstruction

Final remarks

Further work:

- Using these new transforms in practical algorithms (MRI, Electron microscopy, ...). Not an obvious or easy task!
- 3D: discretization of the sphere, rotating spheres, etc.
- Directional bases suitable for numerical applications
- Near optimal grids in "arbitrary" domains for functions bandlimited in a disk